Chapter 1

Fundamentals

Sixty years ago, satellite meteorology did not exist except perhaps in science fiction. Today, satellite images of the world's weather, animated sequences of tropical storms, 5-day weather forecasts, are all being beamed through satellite channels into our television sets every hour or half-hour. Anyone, not just meteorologists, can access the latest images scanned by meteorological satellites around the world, through PCs connected to the internet or even mobile phones. The fascinating origin of satellite meteorology as an independent branch of the science of meteorology, and its phenomenal growth, have indeed had a touch of fantasy. What satellite meteorology happens to be today, is the result of an interplay of science on one hand, and the technology of satellites, computers and communications on the other. Limitations of technology have been overcome by scientific ingenuity, and the requirements of science have driven technology to the cutting edge.

After the successful launch of the first weather satellite in 1960 and the growth of satellite coverage of the earth's atmosphere and oceans within just a decade afterwards, meteorologists were in fact overwhelmed by the new satellite data that became available to them. Prior to the satellite era, meteorologists had laid the greatest emphasis on atmospheric pressure. Lows and highs showing up in synoptic isobaric analysis were of their main interest and many other weather elements including cloud cover, although observed, were not analysed on a synoptic scale in a similar manner. With the availability of satellite images, however, the accent shifted to observing and examining clouds and cloud patterns in the imagery, from which the state of the atmosphere could be directly observed or inferred. Images received from geostationary and orbiting satellites together revealed the presence of a wide spectrum of atmospheric phenomena across individual cumulus cells, thunderstorms, tropical cyclones and jet streams, just at a glance. So much so, that ground weather observation stations began to face the risk of redundancy and closure. Competition from satellite imagery forced many national meteorological services to take a re-look at their network configurations and trim them, particularly the upper air stations which are expensive to operate and maintain.

While the question whether meteorological satellites can give us all that we want for weather analysis and forecasting has been a subject of debate, the answer as of now at least, appears to be firmly in the negative. In spite of the limitations of conventional data and the clear advantages of satellites, the global ground observing network cannot just be done away with. Over land, the atmospheric pressure at the surface is measured most accurately with barometers and automatic instruments. This is the data on which all synoptic weather charts are constructed. Over the sea, pressure data is very sparse. However, as of now, atmospheric pressure cannot be retrieved from satellites, except that low pressure areas can be identified in a qualitative sense from certain cloud patterns in satellite imagery. It has not so far been possible to re-create a synoptic weather chart with remote sensing data alone.

The greatest help from weather satellites comes in observing weather over oceans, mountains, deserts, and unpopulated places where conventional data is either sparse or just unavailable. Here again, satellite data may not be able to replace the functions of an observing network for various reasons. For example, ship observations of sea surface temperature are made within the upper 1 m layer of the sea, while only the ocean skin temperature is retrieved from satellites, and it has errors associated with it due to the presence of clouds and atmospheric moisture. On ground, temperature measurement is made at 1.4 m height above the ground in a Stevenson Screen. It is extremely difficult to get this from satellites as the emissivity of land is highly variable and is not accurately known.

Over land, accurate measurements can be made with anemometers and automatic instruments and over sea, ships and buoys provide surface wind data. The popularly used cloud drift technique applied to satellite imagery cannot be used at the surface, but sea surface winds can be obtained from scatterometers.

An observer on the ground looks up to the sky and estimates visually how much of the sky above is occupied by clouds (expressed in 1/8ths of the hemisphere or oktas). Cloud amount has a different meaning when seen from a satellite looking down and becomes the fraction of an area covered by cloud within a prescribed area as seen from the satellite. From the ground, it is the height of the cloud base that can be estimated by an observer or determined by instrumental methods and vertical growth of cloud cannot be visualized. On the contrary, satellites can give the height of the cloud top and help in seeing the vertical growth of clouds from the fall in temperature over time.

Rainfall is measured over land with raingauges and automatic instruments as a point measurement and areal averages are difficult to obtain. Over sea,

rainfall measurements are rarely available. From satellite data, large-scale rainfall can be estimated from the type of cloud, its persistence and assumed rain rate and areal averaging is easy. A space-borne precipitation radar can make direct measurements of rainfall over the sea.

Upper level winds are routinely measured with pilot balloons, radiosondes, wind profilers and radars. Balloon ascents are taken at the most 2-4 times a day due to the high cost of consumables. By using successive cloud imageries, winds can be estimated from the movement of cloud tracers. Here, the availability of suitable tracers determines whether the winds can be derived or not and the derivation process is prone to errors.

Temperature and humidity profiles of the atmosphere are routinely obtained from the global radiosonde network. It is becoming increasingly expensive to run upper air stations, and over the sea only a few ships make radiosonde measurements. Vertical profiles of temperature and humidity are being made globally with sounders on satellites, but the retrieval is a complex process and there are many problems particularly over hot and humid tropics.

In essence, the practices of weather analysis and forecasting currently in vogue employ a judicious combination of conventional and remotely sensed data, so as to compensate for the deficiencies of one source of data with the advantages of the other. The capability of weather satellites to observe and monitor weather systems is determined by various factors such as the number, type and resolution of spectral channels of the radiometer, the period of the satellite orbit which determines its revisit time, its height above the earth, the inclination of the orbit that delineates the geographical coverage, and so on.

1.1 Principles of Meteorological Remote Sensing

Remote sensing has been defined in various ways, but it is basically the process of observing an object in wavelengths that the human eye cannot perceive. The term has also developed a strong association with satellites, although aircrafts can be used for the same purpose. Remote sensing has applications in many diverse areas, ranging from monitoring of earth resources to medical diagnosis, but the basic principles are the same. In the forthcoming sections we shall discuss various aspects of remote sensing as applied to the area of satellite meteorology.

1.1.1 Absorption, Emission, Reflection and Scattering

It is quite a paradox that the radiative and thermal equilibrium of the earth-atmosphere system is not controlled by the two major constituents of the

atmosphere which are nitrogen and oxygen, but by a few of the numerous miscellaneous gases that all put together make up for just 1 % of its volume. The behaviour of gases like water vapour, carbon dioxide, ozone, methane and other trace gases, and also particulate matter floating in the atmosphere, is what alters the radiation from the sun traversing the atmosphere and the radiation returned to space by the earth. Since satellite remote sensing is essentially the measurement of the returned radiation, it is important to know how the gases in the atmosphere influence the radiative processes in the atmosphere.

Atoms and molecules in a gas have electronic, rotational or vibrational energy, and absorption or emission of radiation takes place when there is a transition from one energy state to another. Absorption spectra of atoms, such as atomic oxygen and nitrogen, are associated with electronic transition and occur in the ultra-violet (UV) region of the electromagnetic spectrum. Tri-atomic molecules like those of water vapour, carbon dioxide and ozone, have additional rotational and vibrational transitions, which occur mainly in the infra-red (IR) region. In the visible (VIS) region, gases in the atmosphere account for very little absorption. The main absorption bands are those of three atmospheric gases: water vapour at 6.7 μ, carbon dioxide 15 μ and ozone 9.6 μ (1 μ or micron = 10^{-6} m). There are other minor absorption bands attributable to methane, nitrous oxide, and other gases.

Radiation from the sun gets reflected when it strikes a plane surface such as the ground or cloud tops and its direction gets altered. Depending upon the albedo or reflectivity of the surface, some part of the radiation will be reflected and the remaining amount will get absorbed by the medium or be transmitted through it. Snow and cumulonimbus cloud tops have high albedo values while the ocean surface reflects very little of the radiation falling upon it.

Air molecules and suspended particles or aerosols scatter radiation in the VIS wavelengths. When the size of the scattering particles is small compared to the wavelength of the incident radiation, the scattering is said to be of the Rayleigh type. In Rayleigh scattering, the intensity is inversely proportional to the fourth power of the wavelength, and the distribution of scattered radiation intensity is symmetric in both the forward and backward directions. When the sizes of the scattering particles become comparable to the wavelength of the incident radiation, the scattering processes is said to be of the Mie type, in which the angular distribution of the scattered radiation intensity is complex and asymmetric. Rayleigh scattering by air molecules is what gives the blue colour to the sky, while Mie scattering by the larger sized particles and aerosols gives it a grayish appearance.

1.1.2 Black Body and Radiation Laws

Many fundamental laws governing the absorption and emission of electromagnetic radiation are commonly based on the concept of what is termed as a black body. This is largely a theoretical concept as ideal or perfect black bodies can be said to be almost non-existent. A black body is defined as an object that absorbs all radiation incident upon it, does not reflect any of it, and emits all energy at full efficiency for all wavelengths as per the following equation

$$B\ (\lambda,T) = 2hc^2\lambda^{-5} / (e^{hc/\lambda kT} - 1)$$

where B is the energy in w m^{-2} μ^{-1},
T is the temperature of the black body in ºK,
λ is the wavelength in μ,
h is Planck's constant 6.625×10^{-27} erg sec,
k is Boltzmann constant 1.38×10^{-16} erg ºK^{-1},
c is the velocity of light 3×10^{10} cm sec^{-1}

This relationship of the black body emission to its temperature is known as Planck's Law. For any given temperature, Planck's Law gives a distribution of emitted energy or a characteristic spectrum of electromagnetic radiation that peaks at a certain wavelength. This peak shifts to shorter wavelengths for higher temperatures and the area under the curve grows rapidly with increasing temperature.

Wien's Displacement Law describes the temperature dependence of the black body radiation curves derived from Planck's Law and it states that the wavelength λ_{max} at which the black body radiation is the maximum is inversely proportional to the temperature T of the black body (in ºK), or

$$\lambda_{max} = c / T$$

where c is a constant whose value is 2898 μ ºK.

Stefan-Boltzmann's Law gives the total energy E emitted at all wavelengths by the black body at temperature T,

$$E = \sigma T^4$$

where σ is the Stefan-Boltzmann constant which has a value of 5.6705×10^{-5} erg cm^{-2} sec^{-1} ºK^{-4}.

E is in fact the area under the Planck's Law curve.Thus, as the temperature of a black body increases, the shift of the peak emission to shorter wavelengths is governed by Wien's Law while the increase in the height of the curve is explained by Stefan-Boltzmann's Law. This increase in E with temperature is not linear, since it varies with the fourth power of the temperature.

There is another important law called Kirchhoff's Law which states that the ratio ε of emitted radiation to absorbed radiation is the same for all black bodies at the same temperature. This law forms the basis for the definition of emissivity. The emissivity of a perfect black body is 1 and that of a perfect reflector is 0.

Strictly speaking, the laws mentioned above are applicable only to a black body, but they are important in the real world as they can be applied as a close approximation to other bodies which have a very weak interaction with the surrounding environment and can be considered to be in a state of equilibrium. In the earth-atmosphere system, the earth's sea surface and thick clouds can be regarded as acting very similar to a black body.

1.1.3 Solar and Terrestrial Radiation

The radiation laws described in the previous section help us to understand the nature of an object and identify some of its thermal properties by interpreting the pattern of radiation emitted by it in different wavelengths. The spectrum of the solar radiation received at the top of the earth's atmosphere matches very well the spectrum of a black body having a surface temperature of about 5700 ºK. This is called solar radiation and it has a peak at about 0.5 μ (Figure 1.1.3.1). The radiation emitted by a black body at the same temperature as the average temperature of the earth's surface which is 283 ºK, peaks at about 10 μ (Figure 1.1.3.2). We therefore have to deal with two different radiation regimes, the radiation received by the earth from the sun, called solar or shortwave radiation and the radiation returned to space by the earth-atmosphere system, called terrestrial or infra-red or longwave radiation. The intensity of terrestrial radiation is far less than that of solar radiation.
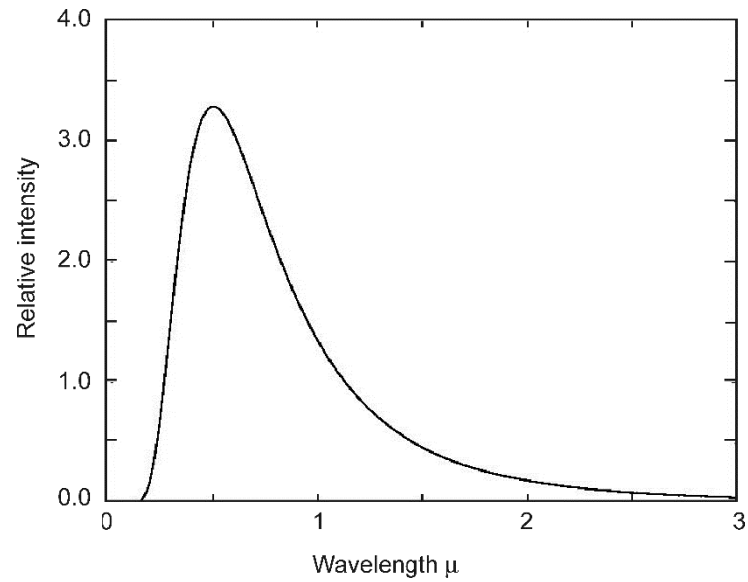
Figure 1.1.3.1 Variation of the relative intensity of black body radiation with wavelength (μ) at temperature 5700 °K, peaking at a wavelength of 0.5 μ in the visible region (Solar radiation)
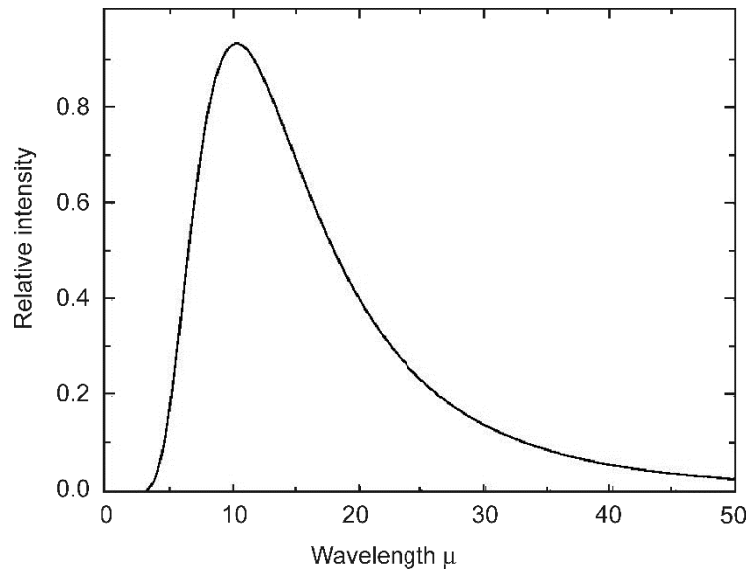

Figure 1.1.3.2 Variation of the relative intensity of black body radiation with wavelength (μ) at temperature 283 °K, peaking at a wavelength of 10 μ in the infrared region (Terrestrial radiation)

1.1.4 Sun-Earth-Atmosphere Radiation Budget

The solar constant is defined as the annual average solar radiation received outside the earth's atmosphere on a plane normal to the incident radiation at the mean sun-earth distance and has a value close to 2 cal cm^{-2} min^{-1} or 1370 W m^{-2}. The actual solar irradiance varies by 3-4% of this value during the year due to the eccentricity of earth's orbit about the sun.

If we consider the incoming solar radiation at the top of the atmosphere as made of 100 units, 30 units are reflected back to space (6 by the atmosphere, 20 by clouds and 4 by the earth's surface). 19 units are absorbed by the atmosphere (16 by gases and 3 by clouds). The remaining 51 units are absorbed by the earth's surface.

Out of these 51 units, 6 are lost to space directly and 45 are returned upwards and absorbed by the atmosphere and clouds (7 by convection and conduction, 23 by evaporation as latent heat and 15 by longwave radiation). The atmosphere and clouds have already absorbed 19 units from the solar radiation, making a total of 64 units which are returned to space as longwave radiation. The budget is thus balanced at the top of the atmosphere.

At the earth's surface and at any level in the atmosphere, the net radiation is the balance of four radiative fluxes, downward solar radiation, downward longwave radiation, upward solar radiation and upward longwave radiation. These can be measured with special instruments installed on the ground or flown on balloons as radiometersondes. The prime factors involved in the radiation budget of the earth-atmosphere system are the albedo or reflectance properties of land, ocean and cloud tops, scattering properties of aerosols, dust and particulate matter in the atmosphere, and vertical profiles of temperature and concentration of gases which absorb longwave radiation (water vapour, CO_2, ozone). Data on these variables if available can be used to compute the radiation budget components indirectly.

1.1.5 Electromagnetic Spectrum

By the term spectrum, we traditionally mean the seven colours of visible light, such as those seen in a rainbow. Nowadays, the term has come to be associated more with mobile communications. In scientific parlance, however, it refers to the entire range of wavelength or frequency of electromagnetic radiation, visible light or the microwave region being just small parts of it (Table 1.1.5.1). The characteristic spectrum of a given object is the pattern of electromagnetic radiation that it absorbs, transmits and emits.

The product of the wavelength λ and frequency ν of electromagnetic waves is equal to c, the velocity of light. The associated energy $E = h.\nu = h.c / \lambda$ where h is Planck's constant. This means that as the wavelength of electromagnetic radiation increases, its frequency decreases and the associated energy gets reduced.

The region of the electromagnetic spectrum with which we are most concerned in real life is the region of visible light, to which the human eye is very sensitive and in which the sun and stars emit the strongest radiation. In recent times, we are getting familiar with other wavelength regions as FM radio stations, mobile phones, satellite television or microwave ovens become more and more a part of our daily life.

Table 1.1.5.1 Electromagnetic Spectrum

Wavelength		**Wavelength**	
10^{-6} nm		1 mm	Millimetre Waves (mm)
10^{-5} nm	Gamma Rays (MeV)	1 cm	Microwaves (cm, GHz)
10^{-4} nm		10 cm	
10^{-3} nm		1 m	
10^{-2} nm		10 m	Radio Waves (MHz, kHz)
10^{-1} nm	X-Rays (Å)	100 m	
1 nm		1 km	
10 nm		10 km	
100 nm	Ultra-Violet (nm),	100 km	
1 μ	Visible, Near Infra-Red(μ)	10^3 km	
10 μ	Thermal Infra-Red (μ)	10^4 km	
100 μ	Far Infra-Red (μ)	10^5 km	

Note: 1 nm (nanometre) = 10^{-9} m and 1 μ (micrometre or micron) = 10^{-6} m

Table 1.1.5.2 Wavelength Range of Visible Colours

Colour	**Wavelength**	
	(nm)	**(μ)**
Violet	380-430	0.38-0.43
Indigo	430-500	0.43-0.50
Blue	500-520	0.50-0.52
Green	520-565	0.52-0.565
Yellow	565-590	0.565-0.59
Orange	590-625	0.59-0.625
Red	625-740	0.625-0.740

The seven colours of the visible spectrum are identified by their wavelengths (Table 1.1.5.2). Radiation of wavelengths shorter than violet is called ultra-violet (UV) radiation. This has very high energy that can break chemical bonds, ionize molecules, damage skin cells or cause cancer. However, most of the UV radiation coming from the sun is absorbed by the layer of atmospheric ozone which resides in the stratosphere, and shields life on earth from its harmful effects.

X-rays have wavelengths that are even shorter than UV, which are expressed in Å (Angstrom Units or 10^{-10} m). Gamma rays have wavelengths that could be as short as 10^{-15} m and it is more convenient to express their magnitude in terms of their energy levels which are of the order of KeV (Kilo electron volts) or MeV (Million electron Volts). X-rays and gamma rays have great penetration power and have applications in astronomy, radioactivity and other fields.

Towards the other end of the visible spectrum, radiation which has wavelength higher than red is called infra-red (IR). The IR region of the spectrum can be further sub-divided into near (NIR), short-wave (SWIR), middle (MIR), and thermal (TIR) with increasing wavelength.

Radiation with still longer wavelengths are called millimetre waves, followed by microwaves and radio waves. These again are further classified with respect to their frequency as given in Tables 1.1.5.3 and 1.1.5.4.

Table 1.1.5.3 Nomenclature of Microwave and Radio Wave Frequencies

Abbreviation	Full Form	Frequency	Wavelength
EHF	Extremely high frequency (Microwaves)	30-300 GHz	1 mm-1 cm
SHF	Super high frequency (Microwaves)	30-3 GHz	1 cm-10 cm
UHF	Ultra-high frequency	3 GHz-300 MHz	10 cm-1 m
VHF	Very high frequency	300-30 MHz	1 m-10 m
HF	High frequency	30-3 MHz	10 m-100 m
MF	Medium frequency	3 MHz-300 kHz	100 m-1 km
LF	Low frequency	300-30 kHz	1-10 km
VLF	Very low frequency	30-3 kHz	10-100 km
VF	Voice frequency	3 kHz-300 Hz	$100-10^3$ km
ELF	Extremely low frequency	300-30 Hz	10^3-10^4 km

Table 1.1.5.4 Microwave Bands

Band	Wavelength	Frequency
mm-Band	1-7.5 mm	40-300 GHz
Ku-K-Ka- Band	0.75-2.5 cm	12-40 GHz
X-Band	2.5-4 cm	8-12 GHz
C-Band	4-8 cm	4-8 GHz
S-Band	8-15 cm	2-4 GHz
L-Band	15-30 cm	1-2 GHz

1.2 Satellite Orbits

The design of an optimum orbit around the earth for a meteorological satellite is a complex process. There are two main classes of orbits, polar orbiting and geostationary, and they are complementary to each other. However, many new types of orbits have now come into use or are being considered. The following sections describe the fundamental principles behind orbit design, technical considerations and the operational implications.

1.2.1 Gravitational and Astronomical Laws

There are certain classical laws that were originally formulated to explain the motion of planets in the solar system and their orbits around the sun. They are, however, very fundamental and general in nature and we now know that they are equally applicable to the orbits of artificial satellites placed around the earth and other planets or moons in the solar system.

Kepler's laws of motion state that: (i) A planet moves around the sun in an elliptical orbit, with the sun at one focus, (ii) The vector joining the sun's centre to the planet sweeps out equal areas in equal time, and (iii) The square of the period of revolution of the planet is proportional to the cube of its semi-major axis. As mentioned above, these laws also hold good for artificial satellites orbiting the earth.

Kepler's laws have to be considered in conjunction with another fundamental physical law. As per Newton's law of gravitation, the gravitational force between two bodies of mass m_1 and m_2 is proportional to the product of m_1 and m_2 and inversely proportional to the square of the distance r between them, or

$F = G\, m_1\, m_2\, /r^2$

where G is the universal gravitational constant having a value of 6.67×10^{-8} $cm^3 g^{-1} sec^{-2}$.

The forces acting on a satellite around the earth are the gravitational force and the centripetal force, which should balance for the satellite to attain a stable orbit. So we must have

$$m_s v^2 /R = GM_e m_s /R^2$$

where M_e and m_s are the masses of the earth and satellite respectively, R is the mean distance between them and v is the velocity of the satellite. The term m_s appears on both sides of the equation and can be cancelled out. We then have

$$v^2 = GM_e /R$$

For a circular orbit, the velocity v can be expressed as $2 \pi R / T$ where T is the time period of revolution of the satellite, which is inversely related to its mean distance from the earth and is given by the equation

$$T^2 = 4 \pi^2 R^3 /GM_e$$

This means that the time period, speed and acceleration of an artificial satellite orbiting the earth are not dependent upon its mass. So theoretically speaking we can put into orbit as big a satellite as we wish, the only practical constraint being that of lifting it into space with the rockets that we have.

It needs to be clarified here that the centripetal force is not independent but derived from the continuous gravitation-related fall of the satellite. However, that does not mean that the gravitational force can on its own sustain the satellite stability. Orbits begin to decay slowly with time and the imbalance of forces may need to be occasionally corrected by firing on-board thrusters.

We can evaluate T for a given R as

$$T = (4 \pi^2 R^3 /GM_e)^{1/2}$$

R can be expressed as $R_e + h$, where R_e is the radius of the earth and h is the height of the satellite above the earth. For the limiting case of h = 0, and using $M_e = 5.98 \times 10^{24}$ kg, and $R_e = 6370$ km, T works out to be 84 min. In reality of course it is not possible to have a satellite grazing the earth. For

h = 200 km, T will work out to be 88 min. For h = 1000 km, T will be 105 min, and this is a popular choice for meteorological satellites.

If T is set at 24 hr, the height of the satellite will work out to be about 35,840 km above the earth's surface. Such an orbit is called geosynchronous as the satellite matches the angular velocity of the earth at this height.

1.2.2 Orbital Elements

As depicted in Figure 1.2.2.1, the satellite's orbit is specified by the following parameters (Kelkar et al 1980):

(a) a - the semi-major axis of the orbit (defines the size of the orbit)
(b) e - the eccentricity of the orbit (defines the shape of the orbit)
(c) I - the inclination of the orbit (with respect to the earth's equatorial plane)
(d) Ω - the right ascension of the ascending node (longitude of the north-bound equatorial crossing)
(e) ω - the argument of the perigee
(f) f - true anomaly
(g) T_e - epoch time

For a given orbit, all the above parameters are fixed, except f which specifies the position of a satellite at a given time.

The semi-major axis a of the ellipse is the maximum height of the satellite above the earth's surface. As per Kepler's third law, satellites move faster when they are close to the earth and slowly when they are further away. The semi-major axis is thus an indirect measure of the average speed or mean motion of the satellite.

The satellite orbit is generally an ellipse. The eccentricity e is an indicator of the shape of the ellipse. A circular orbit is a special case of an ellipse when e is 0, and as e increases towards the limiting value of 1, the ellipse becomes more and more eccentric or elongated.

The point where the satellite is closest to the earth is called the perigee, and the point where it is farthest from earth is called the apogee. The major axis of the ellipse is thus the line joining the perigee and the apogee. The argument of perigee ω helps to define the orientation of the orbital ellipse within the orbital plane. It is the angle measured at the centre of the earth from the ascending node to the perigee.
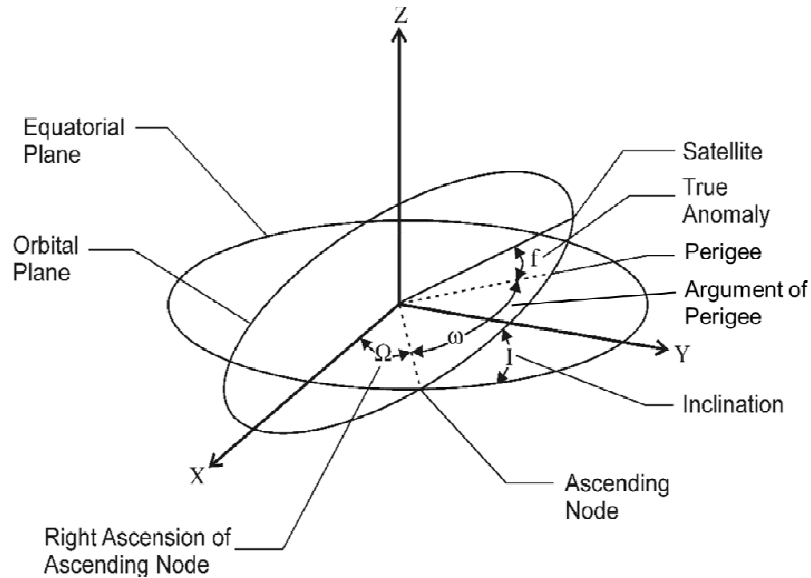
Figure 1.2.2.1 Orbital elements of a satellite in orbit around the earth

For a given inclination, there can be an infinite number of orbital planes. The intersection of the equatorial plane and the orbital plane is known as the line of nodes. The right ascension of the ascending node along with the inclination uniquely specifies the orbital plane. The ascending node is the longitude at which the satellite crosses the equator while going from south to north. The descending node is where the satellite crosses the equator while going from north to south. Since the earth is spinning, we cannot use the common latitude/longitude coordinate system to specify where the line of nodes points. Instead, we use an astronomical coordinate system, known as the right ascension/declination coordinate system, which does not spin with the earth. Right ascension is an angle measured in the equatorial plane from a reference point in the sky where right ascension is defined to be zero, which is the vernal equinox. Thus the right ascension of the ascending node Ω denotes an angle, measured at the centre of the earth, from the vernal equinox to the ascending node (see Section 1.4.4).

The true anomaly f is the angle at the centre of the earth, measured in the orbital plane, between the perigee and the satellite at any given time. If the satellite is in a circular orbit and hence moving at a constant speed, this angle would point directly to the satellite.

A satellite orbit may be subjected to small perturbations due to different reasons such as non-sphericity of the earth's geoid leading to gravitational anomalies, gravitation effects of other celestial bodies like the sun, moon or

stars, atmospheric drag, solar radiation pressure and tides. The order of magnitude of these perturbations would depend on the nature of the satellite orbit. For example, geostationary satellites at 36,000 km height would be less prone to atmospheric drag, but more sensitive to the pressure of solar radiation, whereas the reverse would be true in the case of low altitude polar orbiting satellites. Early spacecrafts of the GOES and INSAT series had large solar panels on one side and a long solar sail on the other side for balancing the solar radiation pressure (Figure 1.2.2.2).
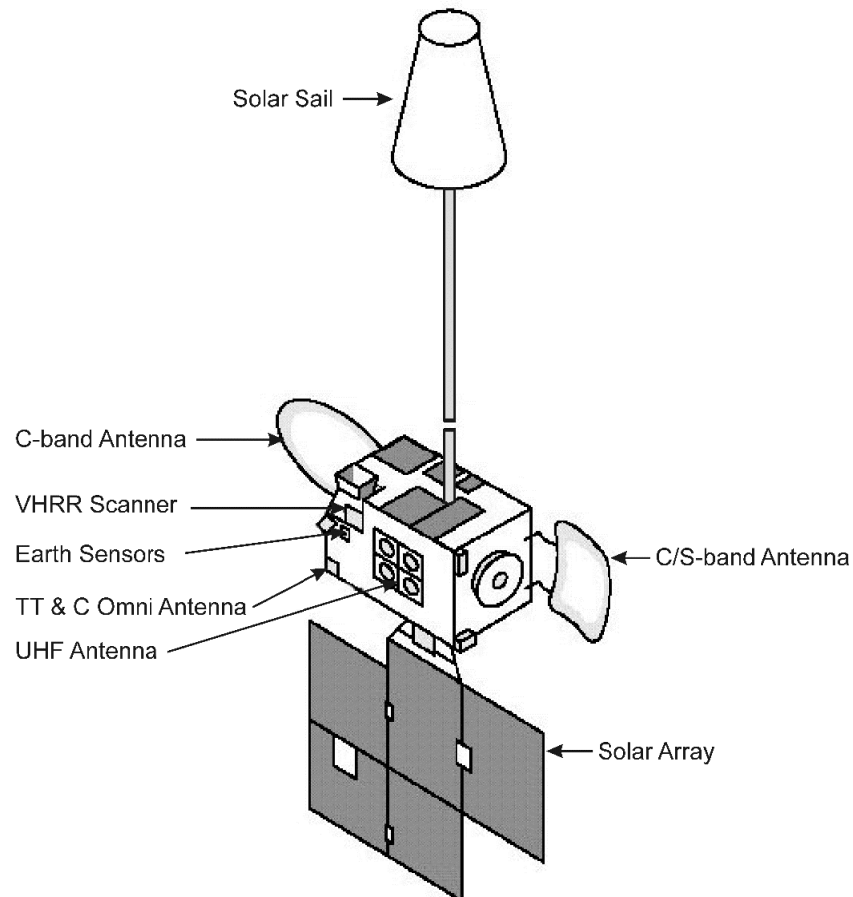

Figure 1.2.2.2 A schematic of the INSAT-1 spacecraft
(Source: IMD)

1.2.3 Types of Orbits

Satellite orbits are generally named after their orbital inclination. For example, if the inclination is 90° the satellite is said to be in a polar orbit. By

definition, a geostationary orbit needs to have an inclination of 0º. For many decades, these were the two preferred orbits for meteorological satellites. It was much later that other inclinations came into use. Megha-Tropiques has a tropical orbit with an inclination of 20º and the GPM core satellite is in an orbit with 65º inclination.

Figure 1.2.3.1 shows the relative orientations of polar, geostationary and tropical orbits around the earth. A satellite in a polar orbit crosses the equator twice a day, but views the poles in every orbit. With every orbital revolution, a new region of the earth comes under its view because of the earth's rotation. A global picture thus emerges over a period of time.

A polar orbiting meteorological satellite is typically in a circular orbit with an altitude of about 850 km and a period of 100 minutes. This results in the satellite scanning a 3000 km wide swath on the earth's surface which can fully cover the polar regions. The satellite completes 14 orbits in a day, and every point on the earth is viewed at least twice a day.
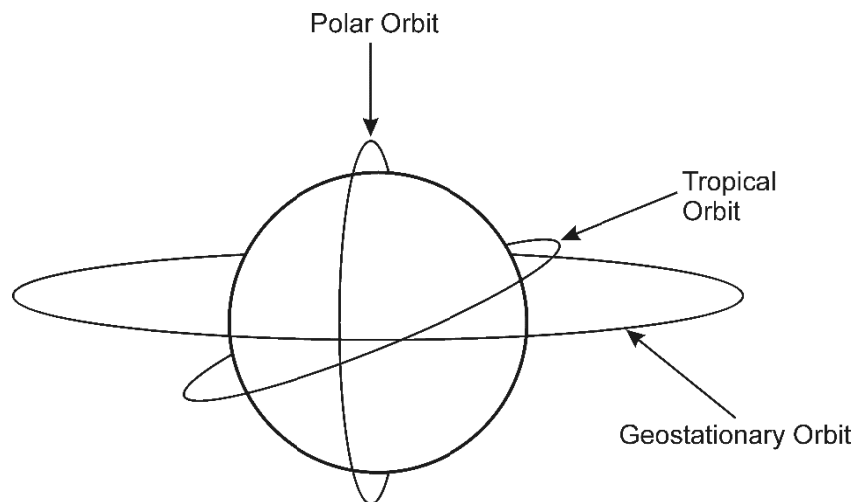

Figure 1.2.3.1 Relative orientations of polar, geostationary and tropical orbits around the earth

The earth is not a perfect sphere and the surface mass is not uniformly distributed, leading to gravitational anomalies. Other bodies in the solar system also exert their gravitational influences on a spacecraft in orbit around the earth. It is possible to choose the parameters of a spacecraft's orbit so as to take advantage of these gravitational influences to induce precession or a slow movement of the satellite orbital plane with respect to fixed inertial space. A special case of a polar-orbiting satellite is a sun-synchronous

satellite which is designed in such a manner that the precession of the satellite orbit matches the earth's revolution around the sun. In other words, the satellite crosses the equator at the same local time (there are AM and PM orbits) and views any given place under comparable lighting conditions. The orbit does not go exactly over the poles but has an inclination of about 100º and a height of 700-1000 km. Occasional orbit maneuvres may be required to maintain the sun-synchronous characteristics of the orbit.

When a satellite is placed in a circular orbit with a radius of 42,400 km or a height of 36,000 km above the earth's surface, it will circle round the earth with the same angular velocity as that of the earth. At that specific height, it will complete one orbital revolution around the earth in 24 hours. Such a satellite is called a geosynchronous satellite. A special case of a geosynchronous satellite is one in which its orbit is in the equatorial plane. In a relative sense, it will appear to remain stationary above a given point on the equator. Such a satellite is called a geostationary satellite and it can provide a continuous earth view from about 80º N to 80º S, but not the polar regions. Practically, however, the useful view is limited to about 60º around the subsatellite point, as the image outside it gets distorted. A constellation of 5 or 6 geostationary satellites spaced around the equator can together give a near-global picture. Geostationary satellites are ideal for communications purposes and continuous monitoring of the weather over the region within their view. Considerations of orbit stability demand that a geostationary satellite be placed only over a point on the equator and not above any other latitude. To maintain the geostationary satellite within the permissible limits of altitude and inclination, station-keeping maneuvres have to be carried out periodically.

When the direction in which a satellite is moving in its orbit around the earth is the same as that of the rotation of the earth, the orbit is called direct or prograde. If the satellite is moving in a direction that is opposite to that of the earth's rotation, the orbit is called retrograde. A geostationary satellite is a special case of a prograde orbit in the equatorial plane, while polar-orbiting satellites are generally placed in a retrograde orbit with an inclination of about 100º. An inclination of 180º would mean a retrograde equatorial orbit.

Kelkar et al (1982) had envisaged a non-geostationary satellite orbiting around the equator and providing frequent meteorological coverage of the entire tropical belt. Such orbits have now become a reality with the launch of the Megha-Tropiques mission (see Section 6.6).

1.2.4 Satellite Attitude

While the altitude of a satellite is its height above the earth, the term satellite attitude refers to its orientation in space. Altitude and attitude are two equally important characteristics of a satellite and they together determine the kind of mission that the satellite can best perform. In the case of a meteorological or remote sensing satellite, the antennas must always remain in ground contact for communications and data transfer, and its imaging sensors must always view the earth as intended. Any deviation from the nominal attitude would result in an improper functioning of the satellite. Satellite attitude therefore demands to be carefully controlled and the two ways of doing it are through spin-stabilization and three-axes stabilization.

A spin-stabilized satellite rotates around its own vertical axis, spinning like a top and resisting external perturbation forces. Here the orientation of the satellite spin vector in space defines its attitude. Spin-stabilized satellites are equipped with thrusters which can be fired occasionally to bring about desired changes in the spin rate and to restore the spin vector orientation. The early GOES and Meteosat satellites had a cylindrical design and rotated at the rate of one revolution per second during which the earth's disc would be scanned. A disadvantage in spinning satellites is that they cannot have large solar arrays and require to be supported by battery power. Another inconvenient factor is that instruments or antennas are required to de-spin so that the antennas and radiometers maintain their desired orientation relative to the earth.

The first Indian National Satellite, INSAT-1A, launched in 1982, was different from the U. S. and European satellites operating at that time, in that it was a non-spinning satellite, a concept that was later adopted by many other countries including the U. S. In a non-spinning satellite, the attitude is defined in terms of the deviations from the nominal orientations of its roll, pitch and yaw axes. The terms roll, pitch and yaw are applied to a satellite in the same manner as they are used in the case of ships or aircrafts. Roll is the rotation of the spacecraft around the direction of its forward movement. Yaw is its rotation around the axis looking at the nadir. Pitch is the rotation around an axis normal to the roll and yaw axes. The three axes can be envisaged as lines running through the satellite's centre of gravity and intersecting at right angles.

The attitude of non-spinning satellites is controlled by minimizing the roll, pitch and yaw. This is called three-axes stabilization, and achieved through the deployment of electrically powered spinning wheels called momentum or reaction wheels. These wheels are mounted in three orthogonal axes on the

spacecraft and allow a transfer of angular momentum back and forth between the spacecraft and wheels. If the satellite is found to be deviating from its desired attitude, the appropriate spinning wheels are speeded up or slowed down to restore the correct attitude. Spacecrafts may also have propulsion system thrusters to apply the required torque. An advantage of three-axes stabilization is that radiometers and antennas can always be made to point at the desired targets without having to perform de-spin maneuvres.

In three-axes stabilized geostationary meteorological satellites, the scanning radiometers have to alternate their scans between east-west and west-east directions until the earth's disc gets fully scanned. The polar-orbiting NOAA satellites are also three-axes stabilized but the scanning is required to be done only in the east-west direction as the north-south progression of the scan is taken care of by the movement of the satellite in its orbit.

Attitude errors result in a distortion of the satellite image and the scene viewed looks slightly different from the nominal view. Yaw errors will result in the image getting rotated around the sub-satellite point in a clockwise or anticlockwise manner. With roll and pitch errors, the image will not be centred at the nominal sub-satellite point but a little away from it. When the attitude errors are large, the sub-satellite point of a geostationary satellite is seen to meander in a figure-of-eight pattern around its nominal position on the equator.

1.3 Meteorological Satellite Payloads

The basic payload carried by the TIROS-1 satellite in 1960 was just a television camera that relayed to the ground whatever it saw of land, ocean and clouds. With every successive meteorological satellite launched over the last six decades by different countries, there have been rapid advances in satellite instrumentation and technology, serving various areas of application, which will be described in the next few sections and the following chapters of this book.

1.3.1 TV Cameras

Historically speaking, the earliest attempt to observe the earth's weather from space was made by the U. S. satellite, Vanguard 2, which was launched on 17 February 1959 but it could not collect much useful data. The world's first meteorological satellite to be considered a success, was the Television and Infra-Red Observation Satellite, TIROS-1, which was launched by the U. S. on 1 April 1960. TIROS-1 was operational for only 78 days, but it demonstrated beyond doubt the tremendous potential use of satellites for

surveying global weather conditions from space and paved the way for future advancements.

TIROS-1 had carried two television cameras, a low-resolution one and a high-resolution one. The pictures were transmitted directly to ground receiving stations. Each camera had a magnetic tape recorder for storing photographs taken when the satellite was out of range of ground stations. The spacecraft was spin-stabilized but not earth-oriented. Therefore, the cameras were only operated while they were pointing at the earth when that portion of the Earth was in sunlight. The video systems relayed thousands of pictures containing cloud cover views of the earth that provided information about large scale cloud regimes for the first time.

TIROS-2 was launched on 23 November 1960 and was operational for over a year. Besides TV cameras, it also carried two experimental infra-red radiation sensors which were successfully used. The TV cameras used 500 scan-line, 1.27 cm vidicons. The tape recorders could store up to 32 frames of pictures. Transmission of the 32-frame sequence was accomplished in 100 sec by a 3 watt FM transmitter. Pictures taken from the satellite altitude of about 700 km by the wide angle camera covered a 1200 × 1200 km area with a spatial resolution of 2.5-3 km at nadir. The narrow angle camera covered a 120 × 120 km area and had a resolution of 0.3 to 0.8 km. The experiment was capable of producing daytime cloud cover pictures for the region between 55 ºS and 55 ºN latitudes. Deposits accumulated on the lens of the wide angle camera caused all its pictures to be of very poor quality. The other camera operated normally until 1 February 1961 and sporadically thereafter until 27 September 1961, but it transmitted more than 25,000 usable pictures.

Five more satellites in the TIROS series were launched during the years 1961 to 1963. TIROS-8 was the first satellite to be equipped with the Automatic Picture Transmission (APT) capability that made satellite pictures available the world over to meteorological agencies in real time as the satellite passed over their region. It was launched on 21 December 1963 and 50 ground stations including one at Mumbai (Colaba) in India, participated in the APT experiment, which was terminated by the end of April 1964 due to degradation of the APT camera. In addition to the APT camera system, the satellite carried a wide angle TV camera which transmitted useful data until 12 February 1966. The satellite was deactivated on 1 July 1967. TIROS-10, which was the last of the experimental satellite series, was launched on 2 July 1965 and had a life of two years.

The successor satellite programme was named after the U. S. agency, the Environmental Science Services Administration (ESSA), which operated it.

The ESSA series was initiated in 1966 as an extension of the TIROS programme and its primary objective was to acquire higher resolution cloud cover images. Over the next four years, nine satellites in the ESSAseries transmitted thousands of images that helped to predict weather patterns including hurricanes. By the end of the programme, more than 300 APT reception stations had come up in 45 countries (Datar et al 1971, Das Gupta 1971).

In 1964, the U. S. National Aeronautics and Space Administration (NASA) launched a parallel satellite programme named Nimbus, to develop observation systems aimed at meeting the research requirements of atmospheric and earth sciences. Between 1964 and 1978, NASA launched seven Nimbus satellites which had very advanced on-board instruments for mapping ozone, sea ice, radiation budget components, coastal zone properties and sea surface temperature, However, Nimbus satellites also continued to carry an improved vidicon camera system for daylight coverage of local cloud conditions which were transmitted through the APT system.

A similar APT service was provided parallelly by the Russian Meteor series of satellites. However, the early satellites in this series were not sun-synchronous and the images were received at different times of the day in each pass.

1.3.2 Scanning Radiometers

After the end of the TIROS satellite series, TV cameras were given up as a means of observing the earth's cloud cover and replaced by scanning radiometers which have became more and more advanced as time went by. Scanning radiometers do not give snapshot pictures but images are constructed from the digital data transmitted by them over a span of time required to complete the scan. In brief, a meteorological satellite measures only radiation. What you see in the satellite image depends upon the spectral band in which the satellite radiometer has received radiation, the sensitivity and response of the sensor, the height from which the satellite is viewing the earth, the time of the scan and such other factors.

The TIROS-N satellite lauched by the U.S. in October 1978, carried a 4-channel radiometer known as the Advanced Very High Resolution Radiometer (AVHRR). This was subsequently improved to a 5-channel instrument (AVHRR/2) that was initially carried on the NOAA-7 satellite aunched in June 1981. The AVHRR/3 with 6 channels was first carried on NOAA-15.

1.3.3 Along Track Scanning Radiometer

Scanning radiometer on polar orbiting satellites generally do the scanning in a direction perpendicular to the satellite's track. As its name indicates, the Along Track Scanning Radiometer (ATSR) is an instrument that has been designed differently and innovatingly for achieving exceptional sensitivity and stability of calibration, enabling measurement of sea surface temperature to an accuracy of 0.3 °K. The first ATSR instrument, ATSR-1, was launched in July 1991 on board the European Remote Sensing Satellite (ERS-1) of the European Space Agency (ESA) as part of its Earth Observation Programme.

The ATSR had one visible channel (1.6 μ) and three thermal IR channels (3.7, 11 and 12 μ) and aimed at achieving a resolution of 1 km. As will be discussed later (see Section 3.5.4), satellite measurements of the temperature of the earth's surface are always vitiated because of the partial absorption of the radiation as it passes through the atmosphere, particularly by water vapour. The ATSR employs a dual view design in order to estimate and correct for these atmospheric effects. The two views result from the instrument's conical scanning mechanism. Each scan takes readings from the nadir position and then sweeps round to take measurements from a point about 900 km along the satellite's track. A few minutes after acquiring the forward view, the satellite passes over the same spot and takes readings for the nadir view. As the two views of the same scene are taken through different atmospheric path lengths, it is possible to calculate a correction for the effect of atmospheric absorption (Stricker et al 1995).

An enhanced version, ATSR-2, was launched on board the ERS-2 spacecraft on 21 April 1995. ATSR-2 was equipped with additional visible channels for vegetation monitoring. The AATSR (Advanced Along Track Scanning Radiometer) instrument was launched on board the ENVISAT spacecraft on 1 March 2002. Mathur et al (2002) have made a validation study of sea surface temperature derived from ERS-1/ATSR observations over the Indian seas.

1.3.4 CCD Cameras

While the use of Charge Coupled Devices (CCDs) has been common in remote sensing satellites for land resources applications, India was the first country to fly a 3-band CCD-based imager in geostationary orbit on its INSAT-2E satellite to complement the VHRR. A similar instrument was also flown on the INSAT-3A satellite. It provides co-registered images of the earth in VIS 0.62-0.68 μ, NIR 0.77-0.86 μ and SWIR 1.55-1.69 μ regions of the spectrum. The ground resolution of these images at the sub-satellite point is 1 km × 1 km for all the three bands. The spectral bands as well as dynamic

range and saturation radiance set points are so selected that the images can be used for meteorological applications as well as vegetation mapping and other earth resources applications. A complete technical description of the INSAT CCD imager has been given by Iyengar et al (1999).

The CCD imager is similar to the VHRR as far as the basic telescope design and scan mechanism are concerned. The separation of the three bands is achieved by two dichroic beam splitters. The first dichroic reflects SWIR energy and transmits VIS and NIR energy, while the second one reflects NIR energy and transmits VIS energy. The VIS and NIR band linear silicon detector arrays are placed directly in the split focal plane of the telescope, whereas an auxiliary lens doublet refocuses the telescope beam to a secondary focus where the SWIR charge coupled photodiode (CCPD) array detector is placed. This optical configuration is designed for achieving identical footprints on the ground while accommodating two different sizes of detector elements. Ground processing is further facilitated by selecting a unidirectional scanning in fast scan direction in view of hybrid scan concept used for this payload. In this type of scanning, mechanical scanning and electronic scanning are simultaneously carried out in two orthogonal axes. This scan geometry generates a three-band image strip of 300 km width (north-south) and 6300 km length (west-east) for each west-east sweep of the scan mirror in 1 min.

Flexible programmable scan modes allow generation of images with up to 24 contiguous strips covering an area of 6300×6300 km on earth. Again, a positioning mechanism enables this image field to be positioned anywhere in a scan field of $20º \times 20º$ covering the full earth disc.

The scan mechanism consists of a gimballed scan mirror which sweeps the composite detector field of view in two orthogonal axes to generate wide-field 2-dimensional imagery. The fast scan sweep of the mirror generates 300 video lines over 6300 km east-west scan every minute. The stepping of the mirror to the south by about 0.4º after each west-east scan helps to generate successive image strips. Earth imaging is done only during west-east scan of the mirror. Scan efficiency is very high as the retrace time is only about 1.25% of active line time. The total scan field of the mirror is $\pm$ 13º east-west and $\pm$ 10º north-south, while the active image field is $\pm$ 5º east-west and a maximum of $\pm$ 5º north-south. This active image field can be positioned anywhere in the total scan field to generate imagery of any part of the visible earth disc.

The detectors used for VIS and NIR bands are 2048-element linear silicon CCD arrays. The outputs of three consecutive detector array elements are added together. Thus 900 pixels of each array are utilized to construct 300 image pixels for each band.

The SWIR detector consists of a 300-element linear CCPD array. This is a hybrid assembly where InGaAs photodiodes are coupled to silicon CCD readout shift registers. As the pixel sizes of VIS/NIR and SWIR CCD arrays are different, effective focal lengths are adjusted by auxiliary optics in SWIR band to give identical ground resolution of better than 1 km × 1km for all the three bands.

Padmanabhan et al (2004) have discussed the complex nature of CCD image processing and the distortions that can arise in the images. They have described the technique of removing the distortions due to the scan imaging, and mosaicing the corrected strips to generate geocoded images of India and the surrounding region. Their method can be used to generate geocoded images of any area imaged by any satellite of the same type. The accuracy of the absolute earth location calculated by considering some ground control points, is found to be about 5 pixels, both in the N-S and E-W directions.

Bhatia et al (1999) have described the wide variety of applications that are possible because to the fine resolution and continuous temporal coverage provided by the INSAT CCD camera.

1.3.5 Spectroradiometers

Precision spectroradiometers are usually based on a monochromator with a diffraction grating. A concave mirror collimates the radiation and the diffraction grating reflects the radiation while dispersing it into its spectral components. A second concave mirror focusses the radiation on a detector. Scanning of the spectrum is accomplished by rotating the grating while recording the electrical signal at the detector.

A satellite-based spectroradiometer can provide extremely high spectral sensitivity with exceptionally low out-of-band response. One such instrument called the Moderate Resolution Imaging Spectroradiometer (MODIS) was flown aboard the Terra and Aqua satellites launched on 18 December 1999 and 4 May 2002 respectively by NASA. Terra's orbit around the earth is timed so that it passes from north to south across the equator in the morning, while Aqua passes south to north over the equator in the afternoon.

Terra MODIS and Aqua MODIS are viewing the entire earth's surface every 1 to 2 days, acquiring data in 36 spectral bands ranging in wavelength from 0.4 to 14.4 μ. The responses are tailored to meet the needs of several applications (Table 1.3.5.1). The resolution at nadir is 250 m for bands 1-2, 500 m for bands 3-7 and 1 km for bands 8-36. A ± 55º scanning pattern at an orbital altitude of 705 km achieves a 2,330 km swath.

Table 1.3.5.1 MODIS Spectral Bands and their Applications

Band	SpectralRange (μ)	Primary Applications
1	0.620 – 0.670	Land/Cloud/Aerosols Boundaries
2	0.841 – 0.876	
3	0.459 – 0.479	Land/Cloud/Aerosols Properties
4	0.545 – 0.565	
5	1.230 – 1.250	
6	1.628 – 1.652	
7	2.105 – 2.155	
8	0.405 – 0.420	Ocean Colour/ Phytoplankton/ Biogeochemistry
9	0.438 – 0.448	
10	0.483 – 0.493	
11	0.526 – 0.536	
12	0.546 – 0.556	
13	0.662 – 0.672	
14	0.673 – 0.683	
15	0.743 – 0.753	
16	0.862 – 0.877	
17	0.890 – 0.920	Atmospheric Water Vapour
18	0.931 – 0.941	
19	0.915 – 0.965	
20	3.660 - 3.840	Surface/Cloud Temperature
21	3.929 - 3.989	
22	3.929 - 3.989	
23	4.020 - 4.080	
24	4.433 - 4.498	Atmospheric Temperature
25	4.482 - 4.549	
26	1.360 - 1.390	Cirrus Clouds Water Vapour
27	6.535 - 6.895	
28	7.175 - 7.475	
29	8.400 - 8.700	Cloud Properties
30	9.580 - 9.880	Ozone
31	10.780 - 11.280	Surface/Cloud Temperature
32	11.770 - 12.270	
33	13.185 - 13.485	Cloud Top Altitude
34	13.485 - 13.785	
35	13.785 - 14.085	
36	14.085 - 14.385	

The scan mirror assembly uses a continuously rotating double-sided scan mirror and is driven by a motor encoder built to operate at 100 percent duty cycle throughout the 6-year instrument design life. The optical system consists of a two-mirror off-axis telescope, which directs energy to four refractive objective assemblies; one for each of the VIS, NIR, SWIR/MWIR and TIR spectral regions to cover a total spectral range of 0.4 to 14.4 μ.

1.3.6 Passive Microwave Sensors

Microwave remote sensing has always been recognized as a powerful tool for meteorological and oceanographic applications, because of its ability to measure water vapour and liquid water even in the presence of most clouds. However, it did not come into popular use due the poor ground resolution of microwave images and because of the fact that land surface emissivity in the microwave region was high and variable. Moreover, microwave sensors have to be flown on low earth orbiting satellites and it has not been possible so far to place them on geostationary platforms because of the weak microwave signal strength. The principles of satellite-borne microwave radiometry have been reviewed by Pandey (1995).

Seasat, Nimbus-5, Nimbus-7 and India's Bhaskara-II, were the earliest satellites to carry passive scanning microwave radiometers and clearly demonstrated the potential of microwave measurements in the retrieval of atmospheric and oceanographic parameters.

Bhaskara-II, which was launched in 1981, carried a Satellite Microwave Radiometer (SAMIR) that had three channels at 19.35, 22.235 and 31.4 GHz, with vertical polarization. The observations were taken close to nadir at angles of 2.8° and 5.6° along the satellite ground trace during each spin of the satellite. The footprint had a size of 240 km. Pathak et al (1992) used SAMIR data for the period January 1982 to June 1983 to derive the latitudinal variation of monthly mean values of atmospheric water vapour content over the Arabian Sea and Bay of Bengal and studied its seasonal and geographical variations. Gohil et al (1982) had earlier derived atmospheric water content from Bhaskara SAMIR data.

Nimbus-5 had the Electrically Scanning Microwave Radiometer (ESMR) operating at a frequency of 19.35 GHz and Nimbus-7 carried the Scanning Multichannel Microwave Radiometer (SMMR).

The Defense Meteorological Satellite Programme (DMSP) is a long term U. S. Air Force effort in space to monitor the meteorological, oceanographic and solar-geophysical environment of the earth. In December 1972, DMSP data

was declassified and made available to the civilian and scientific community. The Special Sensor Microwave Imager (SSM/I), was first flown on the DMSP satellites in June 1987. This was a 7-channel, 4-frequency, linearly polarized, passive microwave radiometric system measuring atmospheric, ocean and terrain microwave brightness temperatures at 19.35, 22.235, 37.0 and 85.5 GHz with footprint sizes varying from 13 × 15 km at 85 GHz to 43 × 69 km at 19 GHz.

Microwave data are used to derive a variety of geophysical parameters such as, ocean surface wind speed, ice cover, cloud liquid water, integrated water vapor, precipitation over water, soil moisture, land surface temperature, snow cover and sea surface temperature. Most of the retrieval algorithms in vogue are in the form of statistical correlations between the brightness temperatures of various channels or differences between channels, with these parameters.

The TRMM Microwave Imager (TMI) on board the Tropical Rainfall Measuring Mission (TRMM) satellite, was a passive sensor operating at 5 microwave frequencies of 10.65, 19.35, 22.235, 37.0 and 85.5 GHz. These frequencies are very similar to those of SSM/I, but TMI had an additional 10.7 GHz channel designed to provide a more linear response for the high rainfall rates in the tropics. All TMI channels had horizontal and vertical polarizations, except the 21 GHz channel which had only vertical polarization. There was 53º conical scanning and the footprints varied in size from 5 km at 85 GHz to 45 km at 10 GHz. TMI had an improved ground resolution resulting from the lower altitude of TRMM (see Section 4.1.1).

The Indian Remote Sensing Satellite IRS-P4 (also known as Oceansat-1) which was launched on 26 May 1999, carried a Multi-channel Scanning Microwave Radiometer (MSMR) operating at 6.6, 10, 18 and 21 GHz frequencies in both H and V polarizations.

1.3.7 Evolution of Meteorological Satellites and Payloads

The TIROS Next Generation satellite programme of the U.S., named TIROS-N, was aimed at providing images and more quantitative environmental data on local and global scales for both day and night with a higher resolution than with the earlier TIROS satellites.TIROS-N was launched on 13 October 1978, and followed by many more satellites in the series, which were later renamed as NOAA satellites, after the operating U. S. agency, the National

Oceanic and Atmospheric Administration. The NOAA satellite series is still in operation but approaching its end with the last satellite in the series, NOAA-19, having been launched on 6 February 2009.

All NOAA satellites are placed in a near-circular polar orbit, and they carry on board an instrument called the Advanced Very High Resolution Radiometer (AVHRR). This was at first a 4-channel radiometer, but it was subsequently improved to a 5-channel instrument (AVHRR/2) beginning with NOAA-7 which was launched on 23 June 1981. The latest instrument version is AVHRR/3, which views the earth in 6 channels, one in visible (VIS), two in near infra-red (NIR), one in mid-wave infra-red (MIR) and two in thermal infra-red (TIR) wavelength regions (Table 1.3.7.1). All the channels have a resolution of 1.09 km at the sub-satellite point.

Table 1.3.7.1 NOAA AVHRR/3 Channel Characteristics

Channel Number	Spectral Band	WavelengthRange (μ)	Applications
1	VIS	0.58 - 0.68	Daytime cloud and surface mapping
2	NIR	0.725 - 1.00	Land-water boundary delineation
3A	NIR	1.58 - 1.64	Snow and ice detection
3B	MIR	3.55 - 3.93	Night-time cloud mapping, sea surface temperature retrieval
4	TIR	10.3 - 11.3	Night cloud mapping, sea surface temperature retrieval
5	TIR	11.5 - 12.5	Sea surface temperature retrieval

(Source:NOAA web site noaasis.noaa.gov/NOAASIS/ml/avhrr)

The instrument utilizes a 20.32 cm diameter collecting telescope. Cross-track scanning across the earth from one horizon to another is accomplished by a continuous 360º rotation of a flat scanning mirror directly driven by a motor. The scan lines are oriented normal to the satellite's direction of movement and the speed of rotation of the scan mirror is selected so that adjacent scan lines are contiguous at the sub-satellite point. Complete strip maps of the

earth from pole to pole are thus obtained as the spacecraft travels in orbit at an altitude of approximately 833 km.

Channels 1 and 2 use silicon detectors, channels 3A and 3B use InGaAs and InSb detectors respectively, while channels 4 and 5 have HgCdTe detectors. The IR detectors are cooled to 105 ºK by a two-stage passive radiant cooler. Although AVHRR/3 is a 6-channel radiometer, at any given time, data of only 5 channels can be transmitted to the ground. Another constraint is that out of the two channels 3A and 3B, only one can operate at a time. All six spectral channels of the AVHRR/3 are well-registered with one another, which means that they all receive radiation from the same spot on the earth at the same time.

The first two geostationary meteorological satellites were SMS-1 and SMS-2, launched by the U. S. on 17 May 1974 and 6 February 1975 respectively. SMS-1 was placed on the equator at 45 ºW over the central Atlantic and SMS-2 at 135 ºW over the east-Central Pacific. Both spacecrafts were spin-stablilised at 100 revolutions per minute. The principle instrument on board was the Visible Infrared Spin-Scan Radiometer (VISSR) which provided day and night imagery of cloud conditions over the earth's disc. The VISSR instrument consisted of a scanning system, a radiometer telescope and VIS and IR sensors, a mirror that was mechanically positioned to provide north-south viewing, while the 100 rpm rotation of the satellite provided for west-east scanning.

The first U. S. Geostationary Operational Environmental Satellite (GOES) was launched on 16 October 1975. GOES-1 to -7 were spin-stabilized satellites and carried the VISSR instrument. GOES-8, the first of a new generation of GOES satellites, was launched on 13 April 1994. Since then, several GOES satellites have been launched. Currently, GOES-13 (or GOES-East) is positioned at 75 ºW longitude, while GOES-15 (or GOES-West) is positioned at 135 ºW longitude.

The new GOES satellites are 3-axes stabilized. The current GOES imager is a 5-channel imaging radiometer. The imager multi-spectral channels can simultaneously sweep an 8 km north-south swath along an alternating east-west and west-east path, at a rate of 20º east-west scan per second. This translates into covering the full earth disc in 26 minutes.

The spectral channels of the scanning radiometers on geostationary satellites are not quite the same as those of the scanning radiometers on polar orbiting satellites. The choice of wavelengths in the VIS, IR and WV bands is made on the basis of several different considerations which apply to the two

different classes of meteorological satellites. Polar orbiting satellites give a composite global mosaic over a course of time and are useful for retrieving the global distribution of parameters like sea surface temperature or vegetation index. They cover the polar regions and are useful for ice cover monitoring. Hence they have near IR and split window TIR channels as described in the previous section. Geostationary satellites are specially suited for continuous monitoring of weather phenomena and large scale atmospheric flows, so they carry a broader VIS channel and a WV channel instead (Table 1.3.7.2).

Table 1.3.7.2 GOES Imager Channels Characteristics

Channel Number	Spectral Band	Wavelength Range (µ)	Resolution (km)
1	VIS	0.55 - 0.75	1
2	SWIR	3.80 - 4.00	4
3	WV	6.50 - 7.00	8
4	TIR	10.20 - 11.20	4
5	TIR	11.50 - 12.50	4

(Source: NOAA web site noaasis.noaa.gov/NOAASIS/ml/imager)

Between1977 and 1997, the European Space Agency ESA and EUMETSAT had launched seven geostationary meteorological satellites of the Meteosat series. The prime Meteosat spacecraft is usually kept positioned at 0º longitude on the equator. In the spring of 1998, METEOSAT-5 was moved to 63º E to cover the Indian Ocean to support the INDOEX programme. The Meteosat has a spinning radiometer which has 3 spectral bands, VIS, WV and TIR, with a wavelength range of 0.45-1.0, 5.7-7.1 and 10.5-12.5 µ respectively. The resolution of the VIS channel is 2.5 km and that of the other two channels is 5 km.

EUMETSAT's Meteosat Second Generation (MSG) satellite (Schmetz et al 2002) carries a 12-channel spinning radiometer called SEVIRI, with a 1 km resolution for the VIS band and 3 km resolution for the IR bands. MSG is capable of providing full-disc images every 15 minutes. The 12-channel configuration of SEVIRI includes a new channel in the ozone absorption band, a triple TIR window and three WV channels to serve various new applications (Table 1.3.7.3). The MSG-1 satellite was successfully launched on 28 August 2002. When MSG-1 became operational in 2004, it was renamed as METEOSAT-8. The MSG-2 satellite was launched on 21 December 2005.

The early Japanese Geostationary Meteorological Satellites were known as GMS. The last operational satellite in this series, GMS-5, was launched in 1995. This series was succeded by MTSAT (Multi-purpose Transportation Satellite) or Himawari in Japanese. The three-axes stabilized geostationary satellite MTSAT-1R was launched on 26 February 2005 at 140 ºE and MTSAT-2 was launched on 24 February 2006 as a standby.The MTSAT radiometer has 5 channels, VIS 0.55-0.80 μ, IR1 10.3-11.3 μ, IR2 11.5-12.5 μ, IR3 6.5-7.0 μ and IR4 3.5-4.0 μ with a resolution of 1 km for VIS and 4 km for IR channels.

Table 1.3.7.3 MSG SEVIRI Channel Characteristics

Channel Number	Spectral Band	Wavelength Range (μ)	Applications
1	HRV	0.6-0.9	Cloud texture, winds
2	VIS	0.56-0.71	Cloud over land, winds
3	VIS	0.74-0.88	Cloud over water, vegetation
4	NIR	1.50-1.78	Cloud over snow
5	MIR	3.48-4.36	Low cloud
6	IR 6.2	5.35-7.15	High level water vapour
7	IR 7.3	6.85-7.85	Middle level water vapour
8	IR 8.7	8.30-9.10	Total water vapour
9	IR 9.7	9.38-9.94	Total ozone
10	TIR 10.8	9.8-11.8	Surface and cloud top temperature, winds
11	TIR 12.0	11.0-13.0	Surface temp. correction
12	TIR 13.4	12.0-13.4	Higher clouds

Russia launched its first Geosynchronous Operational Meteorological Satellite (GOMS-1), also known as Elektro-1, on 31 October 1994. It was located at 77 ºE and had a scanning radiometer with two spectral channels, VIS 0.47-0.70 μ with 1.25 km spatial resolution, and TIR 10.5-12.5 μ with 6.25 km spatial resolution.

China's geostationary meteorological satellites are called Feng-Yun-2 (meaning Wind-Cloud). The main payload of FY-2 is a Visible and Infrared Spin Scan Radiometer (VISSR) which obtains hourly full-disc images of the earth, through step action of the scan mirror, in three channels: VIS 0.55-1.05 μ, TIR 10.5-12.5 μ and WV 6.2-7.6 μ. The sub-satellite point resolution is

1.25 km for VIS and 5 km for the other channels. The FY-2C satellite was launched on 19 October 2004 and placed over 105º E longitude.

1.3.8 Indian Meteorological Satellites

The evolution of the Indian space programme and its meteorological component has been described in many reviews (Kelkar 1994, Pandey et al 1994, Joshi et al 2003). In India, the need to have a national meteorological and remote sensing satellite programme to monitor its weather and vast natural resources was realized way back in the sixties by great pioneers and visionaries like Vikram Sarabhai and Satish Dhawan. The successful launches of the first Indian satellite Bhaskara-I in 1979 and its follow-on Bhaskara-II in 1981 were followed by the launch of INSAT-1A in 1982 and INSAT-1B in 1983. The first Indian remote sensing satellite IRS-1A was launched in 1988.

INSAT is India's unique domestic satellite system which was conceptualized to bring in satellite-based services in as many fields as possible in the quickest possible time. The multi-purpose concept of INSAT led to the realization of the full potential of the geostationary satellite system in one stroke. Thus while other countries had dedicated satellites for different purposes, INSAT-1A ushered in a new era in communications, television and radio broadcasting, and meteorology at the same time. While the first APT station had been established in India in 1965, it had given Indian weather forecasters only limited access to satellite imagery. Satellite meteorology may be said to have truly come of age in India with the launch of the first INSAT satellite in 1982.

Table 1.3.8.1 gives the chronology of the evolution of the INSAT meteorological programme. While the INSAT-1 series consisted of multi-purpose satellites, some of the later satellites have not had any meteorological component. On the other hand, METSAT, launched in 2002 and later renamed Kalpana-1, is exclusively dedicated to meteorological imaging. INSAT-3D, which was launched in 2013, is the first Indian satellite to carry a sounder. It is primarily a meteorological satellite and has no communication transponders except for data relay and satellite-aided search and rescue.

The Indian satellites INSAT-1A to -1D, and INSAT-2A and -2B carried a 2-channel Very High Resolution Radiometer (VHRR). The two channels were visible (VIS) 0.55-0.75 μ and thermal infra-red (TIR) 10.5-12.5 μ. Their resolutions at the sub-satellite point were 2.75 and 11 km respectively for INSAT-1A to 1D, and 2 and 8 km respectively for INSAT-2A and 2B. The

INSAT-2E satellite, for the first time carried a 3-channel VHRR with a water vapour channel (WV) 5.7-7.1 μ added to the VIS and TIR channels. The ground resolution of the WV channel was 8 km.

Full details of the INSAT-2A and -2B VHRR instrument have been described by Joseph et al (1994) and subsequent improvements and additions made to the INSAT-2E VHRR have been discussed by Iyengar et al (1999). The VHRR optics assembly basically consists of a telescope, dichroic beam splitter, IR collimating lens, IR relay optics and VIS band optical elements. The incoming radiation is reflected onto an 8 inch (20.32 cm) diameter primary mirror of the reflective telescope by a two-axis gimbal-mounted beryllium scan mirror. A gold film dichroic beam-splitter placed in the converging beam from the secondary mirror of the telescope bifurcates the radiant energy. The VIS energy is transmitted through the dichroic while combined WV and TIR energy is reflected at right angles to the original direction. This allows the radiation from the earth to be channelled to visible and combined IR focal planes simultaneously with high optical efficiency.

The detector configuration for the VIS band consists of two staggered arrays of four silicon photodiodes each. For WV and TIR bands, the detector package contains two sets of dual mercury-cadmium-telluride (HgCdTe) photoconductive detector elements in close proximity to band defining filters. The IR detectors are operated nominally at a precisely controlled low temperature in the range of 105-115 ºK to limit thermally generated noise. A passive radiant cooler is used to cool the IR detector package. One of the detectors in each band is energized, while the other set provides the on-board redundancy. Both sets are identical in function and can be switched on or off through ground command.

The image of the earth is generated by sweeping the instantaneous geometric field of view of the detectors by rotation of the scan mirror-gimbals in two orthogonal axes. For every east-west sweep of the mirror, four contiguous lines of VIS band and one line each of WV and TIR bands are generated. At the end of the sweep, the mirror is stepped south through an angle equivalent to 8 km on the ground and data collection is resumed in the reverse west-east sweep.

Three modes of operation are provided to allow trade-off between area and frequency of coverage. The full frame mode scans the entire earth disc and some space around (20º × 20º) in about 33 min. The normal frame mode coverage in the east-west direction is the same as in the full frame mode, but in the north-south direction, the scan is limited to only 14º, covering the region between 50 ºN and 40 ºS latitudes in 23 min. In the sector scan mode,

the east-west coverage is the same as in the full frame and normal frame modes, but is further limited to a 4.5º scan in the north-south direction which can be completed in about 7 min. The sector can be positioned, through ground command, anywhere in the full scan field in steps of 0.5º in the north-south direction. This mode is particularly suited for rapid repetitive coverage during severe weather conditions.

The dark and cold space views at the east and west ends are used for establishing reference radiance for all the three bands. A full end-to-end calibration of WV and TIR bands is provided by swinging the mirror to view a black body cavity fitted on the inner side of north plate of the instrument. The physical temperature of the black body is accurately monitored by platinum resistance thermometers at five locations and is telemetered through the VHRR data stream. The system response for black body view is available in the video data slot.

Table 1.3.8.1 Chronology of the Evolution of the INSAT Meteorological Programme

Name of Satellite	Launch Date	Meteoro-logical Payload	Channel	Spectral Range (μ)	Resolu-tion (km)
INSAT-1A	10 April 1982	VHRR (Very High Resolution Radiometer)	VIS	0.55-0.75	2.75
INSAT-1B	30 August 1983	VHRR	IR	10.5-12.5	11
INSAT-1C	21 July 1988	VHRR			
INSAT-1D	12 June 1990	VHRR			
INSAT-2A	10 July 1992	VHRR	VIS	0.55-0.75	2
INSAT-2B	23 July 1993	VHRR	IR	10.5-12.5	8
INSAT-2E	3 April 1999	VHRR	VIS	0.55-0.75	2
			IR	10.5-12.5	8
			WV	5.7-7.1	8
		CCD Charge Coupled Device Camera	VIS	0.62-0.68	1
			NIR	0.77-0.86	1
			SWIR	1.55-1.69	1

Table 1.3.8.1 *Contd…*

Metsat/ Kalpana-1	12 September 2002	VHRR	VIS	0.55-0.75	2	
			IR	10.5-12.5	8	
			WV	5.7-7.1	8	
INSAT-3A	10 April 2003	VHRR	VIS	0.55-0.75	2	
			IR	10.5-12.5	8	
			WV	5.7-7.1	8	
		CCD	VIS	0.62-0.68	1	
			NIR	0.77-0.86	1	
			SWIR	1.55-1.69	1	
INSAT-3D	26 July 2013	VHRR	VIS	0.55-0.75	1	
			SWIR	1.55-1.70	1	
			MWIR	3.80-4.00	4	
			WV	6.50-7.10	8	
			TIR	10.3-11.3	4	
			TIR	11.5-12.5	4	
		Sounder	SWIR	3.67-4.59 6 channels	10	
			MWIR	6.38-11.33 5 channels	10	
			LWIR	11.66-14.85 7 channels	10	
			VIS	0.67-0.72 1 channel	10	

1. Satellites in the INSAT-1 series were built in the U.S. as per Indian design and launched from abroad.
2. Satellites in the INSAT-2 series were built indigenously but launched from abroad.
3. INSAT-2E was the first geostationary meteorological satellite to have a CCD payload.
4. Metsat, India's first exclusive meteorological satellite, was launched from Sriharikota by ISRO's PSLV-C4.
5. Metsat was renamed Kalpana-1 on 5 February 2003 in memory of Dr Kalpana Chawla, the India-born American astronaut who died in the U.S. space shuttle Columbia disaster on 1 February 2003.
6. Kalpana-1 located at 74 °E, INSAT-3A at 93.5 °E and INSAT-3D at 82 °E are the current operational satellites.

The design of the VHRR systems on the currently operational Indian satellites, INSAT-3A and Kalpana-1, are similar to the INSAT-2E VHRR.

The INSAT-3D satellite launched on 26 July 2013 is a totally dedicated meteorological satellite carrying an advanced 6-channel imager and a 19-channel sounder. The imager is an improved design of the VHRR instrument flown on the Kalpana-1 and INSAT-3A missions. It is capable of generating the images of the earth in six wavelength bands significant for meteorological observations, namely, visible, shortwave infrared, middle infrared, water vapour and two bands in thermal infrared regions, offering an improved 1 km resolution in the visible (Table 1.3.8.1).

INSAT-3D also carries a newly developed 19-channel sounder, which is the first such payload to be flown on an Indian satellite mission. The sounder has 18 narrow spectral channels in shortwave infrared, middle infrared and thermal infrared regions and one channel in the visible region. The ground resolution at nadir is nominally 10 km for all nineteen channels (Table 1.3.8.1)

1.4 Satellite Imagery

As satellite images started becoming available to meteorologists around the world in the early sixties, the skills of satellite image interpretation developed very rapidly. Until then, knowledge about clouds had been documented into cloud atlases on the basis of what had been observed from the ground or aircrafts. The view from satellite altitudes was, however, completely new and clouds seen by satellites had to be interpreted in an altogether different manner.

It must also be remembered that in the early days of the satellite era, the picture technology was primitive. APT pictures received directly from satellites flying overhead were produced on facsimile chart paper, mostly of inferior quality and liable to fading in a short time. The images many times lacked clarity and hence they had to be examined with great care. However, the technology improved really fast and even photographic paper was mostly done away with, when interactive computer image processing systems became common. Now of course, there are web sites on the internet on which anyone can access satellite imagery in near real time.

1.4.1 Resolution

The term resolution as applied to meteorological satellites assumes a different meaning in different contexts: spatial, spectral, radiometric and temporal, but in each case it is a critical design consideration. While the highest possible resolution is desirable, it is not always possible to attain it and what is realized is a trade-off between several competing factors. A higher resolution also requires extremely high rates of data transfer and an increasingly complex design of both space and ground systems.

What a scanning radiometer views at any instant is called the Instantaneous Field Of View (IFOV) and it is generally considered as the spatial resolution of the imaging sensor. The size of an individual pixel or picture element also depends mainly on the sampling rate and the forward motion of the spacecraft. In a meteorological satellite, the spatial resolution of the radiometer will decide the smallest cloud that can be seen in the image.

The spectral resolution of the sensor is inversely related to the channel bandwidth. A higher spectral resolution and an accurate spectral signature can be obtained by having a large number of narrow bands, rather than one continuous broad band.

The term radiometric resolution is used to indicate the smallest perceptible change in the radiance of various targets that the sensor can discriminate. It is a measure of the signal-to-noise ratio of the sensor. It can also be defined in terms of the ability to resolve temperature difference between targets.

The temporal resolution is an important consideration in operational meteorology because it determines what kind of meteorological phenomena can be viewed by the satellite, as they have different lifetimes. Temporal resolution refers to the elapsed time interval between two successive satellite scans of a given region. This is also called the repeat cycle or repetivity of the orbit.

The temporal resolution is decided by the design of the scanning radiometer as well as the nature of the spacecraft orbit and it has to have a significant trade-off with the spatial resolution. For achieving a finer spatial resolution, the scan has to be made slower and the temporal resolution will get reduced. In a rapid scan, a selected area can be scanned repeatedly, but then other areas will be left out. Satellites meant for monitoring of earth resources or for cartographic applications can have an extremely high spatial and spectral resolution because they can afford to have a long repeat cycle.

1.4.2 Characteristics of Satellite Imagery

Most of the early interpretation schemes used six characteristics to identify clouds in satellite images (Conover 1962), which were:

(1) Cloud brightness relating particularly to the depth and composition,
(2) Texture - whether smooth, fibrous, opaque, or mottled,
(3) Form of elements - whether regular or irregular,
(4) Pattern of elements - associated with topography, air flow, vertical and horizontal wind shear,
(5) Size - both of the patterns and the individual elements, and
(6) Vertical structure - for example shadows thrown below.

In addition, cloud classification schemes were developed on the basis of cloud patterns (Hopkins 1967):
(1) Vertical features:
      (a) Circular or spiral bands,
      (b) Crescent-shaped or comma-shaped cloud masses,
      (c) Quasi-circular cloud masses, and
      (d) Curved or linear bands.
(2) Major cloud bands, in which the length is much greater than the width,
(3) General features:
      (a) Minor bands like cloud streets, jet stream bands, lee waves,
      (b) Cumuliform features, polygonal cells, and
      (c) Stratiform features, fog areas.

Although nowadays most of the picture interpretation work is carried out on image processing computers, and various interpretation aids are available to the analysts, it is necessary to have a basic knowledge of the fundamental characteristics mentioned above and their importance.

It is also important to remember that interpretation of individual satellite images should never be done in isolation, as may happen for example, when one sees a satellite image flashed on a television channel. The day and time of the image, the geographical area covered, the gray scale and enhancement used, must all be known and given due consideration. Other available observational data and synoptic weather charts should also always be referred to. Continuity in time is essential and earlier images should be compared for detecting changes or confirming the interpretation. Images from all available channels should also be compared. The information derived from the VIS, IR, WV and microwave channels is not redundant but complementary, and when all channels are considered together, they help to remove uncertainties or ambiguities in the interpretation process and to identify clouds and surface features uniquely.

Clouds which appear brighter in VIS imagery are those which have a large albedo because of their great vertical extent, high cloud water/ice content and small cloud droplet size. Shallow clouds having low cloud water/ice content and large cloud droplet size appear gray. Thus towering cumulonimbus clouds (Cb) appear the whitest in VIS images whereas thin cirrus can barely be seen (Figure 2.3.1.1).

Small cumulus clouds usually take the form of open hexagonal cells while stratocumulus clouds appear as closed cells. Low level stratus clouds or areas covered by fog can be identified by their uniform brightness and sharp boundaries (Figure 2.6.2.1). Tall cumulonimbus cloud tops can sometimes be identified by the shadows thrown by them on lower cloud layers.

Since convection is the main source of rainfall in the global tropics, in the early years of satellite observation, the distribution of highly reflective clouds (HRC) was considered important and extensively documented (Garcia 1985). Efforts were also made to use the HRC data for estimating precipitation. Mahajan et al (1991) found a good correlation between the monthly HRC frequency and monthly rainfall data over the island stations in Arabian Sea and Bay of Bengal.

The most important advantage of IR imagery is that it is available at any time unlike VIS imagery which is available only in daylight hours. Secondly, IR radiances are a measure of the temperature of the radiating surface. Clouds which appear white in IR imagery are those which have cold cloud top temperatures such as Cb and cirrus clouds. A mature Cb cloud can be further recognized by its sharp edge on the windward side and a fuzzy edge on the other side resulting from the the cirrus plume. The plume may get blown downwind over several hundred kilometres and give an indirect indication of the upper level wind speed and direction (Figure 2.4.5.3).

Clouds in IR imagery do not have the kind of texture that is seen in VIS imagery. IR images cannot discriminate between low clouds and the sea surface or between fog and land surface, because of the absence of sufficient temperature difference.

Like IR imagery, WV imagery is also available at all times. While IR images are produced from radiances received by the radiometer in the thermal window region, water vapour channel imagery is produced from radiances received in the water absorption band centred at 6.7 μ. The stronger the absorption, the higher is the originating level of the emission that ultimately reaches the satellite. As the atmospheric moisture content decreases with height, the main contribution to the radiance received by the satellite comes

from levels in the lower and middle and troposphere. So in WV imagery, the brighter regions are those with high upper tropospheric humidity and the dark regions are those where the upper troposphere is very dry.

While in IR imagery, the brightness of a pixel depends upon its temperature, there is no such simple relationship between moisture and brightness for a WV image. Since clouds also emit some radiation in the WV band, high and deep clouds and Cb anvils show up with equal prominence in VIS, IR and WV imageries (Figures 2.3.1.1 to 2.3.1.3).

Bhatia et al (1999) have described the characteristic features and many potential applications of water vapour imagery in the INSAT-2E 6.7 μ (5.7-7.1μ) channel.

Generally speaking, WV images have a different appearance from that of VIS and IR images. WV images are characterized by the presence of extensive and continuous structures (Figure 2.8.1). Cloud patterns which appear distinct from each other in the VIS and IR images can be recognized as being a part of the same air mass in corresponding WV images. The band structures also provide some indication of prevailing large scale wind patterns like jet stream cores. This information is important over cloudfree regions where cloud motion winds cannot be derived. WV images show moisture boundaries in the form of plumes, or tongues or streams of moisture. These can be of great help in the prediction of heavy rainfall and resultant flash floods.

WV imagery has been found to be useful in understanding the processes that govern the movement of tropical cyclones. It is generally understood that the recurvature of a north-westward moving tropical cyclone occurs under the influence of an approaching upper air trough. WV imagery is able to capture such interactions, and the possibility of recurvature becomes evident through a northward expansion of the moisture envelope of the cyclone as it approaches this trough. On the contrary, if the imagery shows a significant moisture dissipation on the northern side, the cyclone is likely to keep a westward track.

Images from the 85 GHz microwave channel give important clues about weather phenomena that may be missed out in VIS or IR pictures. They can observe the eye in tropical cyclones since the cirrus overcast is transparent at this frequency, while in IR and VIS images of tropical cyclones the eye region is usually covered by abundant cirrus. In the case of weakening cyclones, they can clearly bring out the cloud formations which other channels cannot show because of the lack of contrast between the clouds and the sea surface.

1.4.3 Gray Scale, Enhancement and Pseudocolour Imagery

In satellite images, the brightness of a pixel is usually assigned a value on a scale of 256 points ranging from 0 to 255, which is called the gray scale. The number 0 on the gray scale stands for pure black and the number 255 stands for pure white. This scale is shown as a strip of continuously increasing brightness at the top or bottom of a satellite image for reference. In a VIS image, lower values on the gray scale are seen over oceans because of their high absorption of solar radiation and the value 0 is assigned to the darkest pixels. The higher gray scale values are seen over snow covered regions and thunderstorm cloud tops, with the value 255 corresponding to the brightest pixels. In an IR image, the lower end of the gray scale corresponds to high temperatures and the higher end of the gray scale to low temperatures. In a WV image, lower values of the gray scale correspond to dry regions and higher values to moist regions.

When satellite images taken at different times or by different satellites, or pictures reproduced by different photographic machines, need to be compared, a reference has to be made to their gray scale wedges to avoid drawing unrealistic conclusions.

While the gray scale is basically linear, in order to improve the contrast between individual pixels, a non-linear gray scale may at times be applied to the image. This procedure is called enhancement, as it effectively enhances the original gray scale in some parts and brings out desired features that may have been masked out in the original image. Of course, stretching the gray scale in one part implies that it will get compressed in another part. Thus enhancement of any feature is always at the cost of some other feature. Various enhancement curves can be designed and used for meeting different requirements. For example, in Dvorak's technique (see Section 2.5.4), a step-cum-linear enhancement curve (Figure 1.4.3.1) can be applied to cyclone images to enhance the outer cloud features and separate the class boundaries (Figure 1.4.3.2 and 1.4.3.3).

Pseudocolour imagery is produced by a special kind of enhancement in which parts of the gray scale are not stretched but assigned different colours or shades to bring out the essential features. For example, tall cloud tops can be made to appear as red (Figure 1.4.3.4 - Colour Plate 2), or clear ocean as blue. In pseudocolour images, the possible enhancement choices are much greater and can be effectively used to draw attention to the desired features. Another way of generating false colour images is by combining VIS and IR images. Here as the common features get added and others get subtracted, the combined colour image can be made to highlight the essential features or give a natural look (Figure 1.4.3.5 - Colour Plate 3).
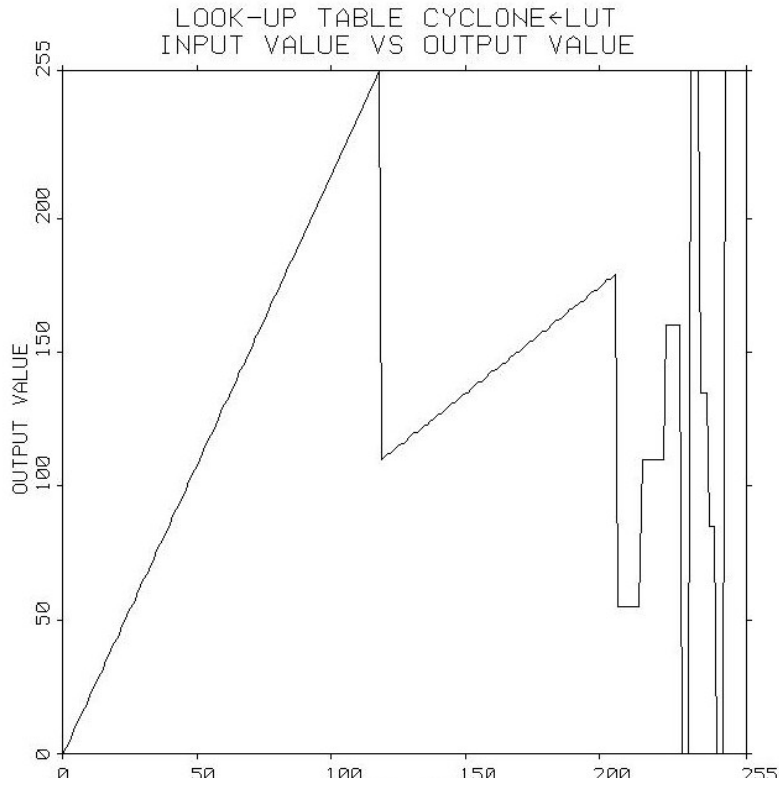
Figure 1.4.3.1 Gray scale enhancement curve for tropical cyclone images
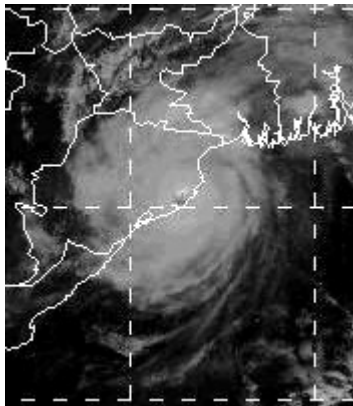(Source: IMD)

Figure 1.4.3.2 Cyclone image
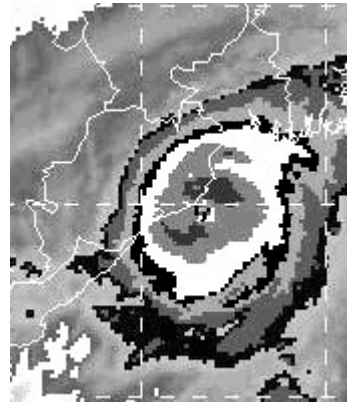without enhancement (Source: IMD)

Figure 1.4.3.3 Cyclone image with
enhancement (Source: IMD)

1.4.4 Navigation and Gridding

Navigation and gridding are two important steps in meteorological satellite data processing and generation of image products. The term navigation is used in its conventional sense and implies the use of landmarks for determination and prediction of orbit and attitude. By this process, it is possible to relate points on the earth, defined by latitude and longitude, to points on the image, given by line and element numbers and vice versa.

By gridding we mean the superposition of grid points, political boundaries or latitude-longitude lines on the navigated image. If geostationary satellite images produced at 30 min interval are viewed in quick succession, the landmarks should appear to be stationary. The removal of apparent earth motion from an animated sequence of images is called registration.

Briefly speaking, the navigation process involves transformations among five different coordinate systems: (a) inertial system, having its origin at the centre of the dynamical earth, and the x-axis pointing to the vernal equinox and z-axis normal to the equatorial plane, (b) rotating system, similar to the inertial system but with the z-axis passing through the Greenwich meridian, (c) local vertical system, having its origin at the centre of the satellite, (d) body-centred system, defined in terms of the pitch, roll and yaw angles, and (e) picture frame system, defined in terms of line and element number (Kelkar et al 1980).

The degree of sophistication of the navigation process determines the accuracy with which the latitude-longitudes of pixels are derived (Prakash et al 1996). This has a very important bearing in quantitative product derivation like cloud motion winds in which the positions of the pixels have to be known very precisely. A poor navigation also shows up as a mismatch between the superimposed grid and the geographical features on the image.

Navigation errors may result in image distortions in various forms such as a vertical compression or expansion of the image, non-vertical alignment of the north and south poles, and multiple representations or omissions of image pixels.

1.5 References

Bhatia R. C., Brij Bhushan and Rajeswara Rao V., 1999, "Applications of water-vapour imagery received from INSAT-2E satellite", *Current Sci*., 76, 1448-1450.

Bhatia, R. C. and Gupta, H. V., 1999, "Use of charged coupled device payload on INSAT-2E for meteorological and agricultural applications", *Curr. Sci.*, 1999, 76, 1444–1447.

Conover J. H., 1962, "Cloud interpretation from satellite altitudes", *Air Force Cambridge Res. Lab., Res. Note No. 81*, 77 pp.

Das Gupta J., 1971, "A stacked Yagi antenna for APT reception", *Indian J. Meteor. Geophys.*, 22, 381-384.

Datar S. V. and Joseph C. P., 1971, "A satellite automatic picture transmission (APT) system ground receiving station", *Indian J. Meteor. Geophys.*, 22, 377-380.

Garcia O., 1985, "*Atlas of highly reflective clouds over the global tropics: 1971-83*", NOAA-ERL, Boulder, Colorado.

Gohil B. S. and co-authors, 1982, "Remote sensing of atmospheric water content from Bhaskara SAMIR data", *Int. J. Remote Sensing*, 3, 235-241.

Hopkins M. M., 1967, "An approach to the classification of meteorological satellite data", *J. Appl. Meteor.,* 6, 164-178.

Iyengar V. S. and coauthors, 1999, "Meteorological imaging instruments on-board INSAT-2E", *Current Sci.,* 76, 1436-1443.

Joseph G. ad coauthors, 1994, "INSAT-2 very high resolution radiometer for meteorological observations", *J. Spacecraft Technol.,* 4, 183-208.

Joshi P. C., Narayanan M. S., Bhatia R. C., Manikiam B., Kirankumar A. S. and Jayaraman V., 2003, "Evolution of Indian satellite meteorological programme", *Mausam*, 54, 1-12.

Kalsi S. R., 2006, "Orissa supercyclone – a synopsis", *Mausam*, 57, 1-20.

Kelkar R. R., Sant Prasad and Ellickson J., 1980, "Image navigation and gridding for three-axis stabilised geostationary satellites", *NOAA/NESDIS Report*, WashingtonDC, 32 pp.

Kelkar R. R., Sant Prasad and Khanna P. N., 1982, "Conception of an equatorial orbiting meteorological satellite for the tropics", *Mausam*, 33, 507-508.

Kelkar R. R., 1994, "Satellite meteorology in India – an overview", *Indian J. Radio Space Phys.*, 23, 235-245.

Mahajan P. N. and Ghanekar S. P., 1991, "Assessment of satellite-observed HRC data for rainfall estimates over the Indian Ocean", *Mausam*, 42, 347-352.

Mathur A., Agarwal V. K. and Panda T. C., 2002, "Validation of ERS-1/ATSR derived SST in Indian waters", *Int. J. Remote Sensing*, 23, 5155-5163.

Padmanabhan N., Ramakrishnan R. and Gurjar S. B., 2004, "Geometric modelling of INSAT-2E CCD payload and multistrip mosaicking for geocoding large areas", Current Sci., 86, 1113-1121.

Pandey P. C. and Kelkar R. R., 1994, "Space Meteorology in India", *Advances in Space Research in India,* Indian National Sci. Acad.

Pandey P. C., 1995, "Satellite-borne microwave radiometry for atmospheric studies", *Indian J. Radio Space Phys*., 24, 245-254.

Pathak P. N. and Gautam N., 1992, "Latitudinal distribution of water vapour over the Arabian Sea and Bay of Bengal using Bhaskara-II SAMIR data", *Mausam*, 43, 385-394.

Prakash W. J. and Bhandari S. M., 1996, "An algorithm to overlay continental boundaries and latitude-longitude grids over INSAT-VHRR images", Computers Geosci., 22, 443-440.

Schmetz J. and coauthors, "An introduction to Meteosat Second Generation (MSG)", *Bull. Amer. Meteor. Soc*., 83, 977-992.

Stricker N. C. M and coauthors, 1995, "ATSR-2: The evolution in its design from ERS-1 to ERS-2", *ESA Bull*., *No. 83*, 32-37.